Proceedings of ASME Turbo Expo 2011
GT2011
June 6-10, 2011, Vancouver, British Columbia, Canada

GT2011-45819

LES OF PRE-VAPORIZED KEROSENE COMBUSTION AT HIGH PRESSURES IN A SINGLE SECTOR COMBUSTOR TAKING ADVANTAGE OF THE FLAMELET GENERATED MANIFOLDS METHOD

Pradeep Pantangi
Department of Mechanical Engineering
Darmstadt University of Technology
Darmstadt, Germany
pantangi@ekt.tu-darmstadt.de

Amsini Sadiki
Department of Mechanical Engineering
Darmstadt University of Technology
Darmstadt, Germany
sadiki@ekt.tu-darmstadt.de

Johannes Janicka
Department of Mechanical Engineering
Darmstadt University of Technology
Darmstadt, Germany
janicka@ekt.tu-darmstadt.de

Michael Hage
Rolls-Royce plc
Derby, United Kingdom
Michael.Hage@Rolls-Royce.com

Andreas Dreizler
Department of Mechanical Engineering
Darmstadt University of Technology
Darmstadt, Germany
dreizler@csi.tu-darmstadt.de

J.A. van Oijen
Eindhoven University of Technology
Mechanical Engineering
Eindhoven, The Netherlands
j.a.v.oijen@tue.nl

Christoph Hassa
DLR, Institute for Propulsion Technology Köln, Germany
christoph.hassa@dlr.de

Johannes Heinze
DLR, Institute for Propulsion Technology Köln, Germany
johannes.heinze@dlr.de

Ulrich Meier
DLR, Institute for Propulsion Technology Köln, Germany
ulrich.meier@dlr.de

ABSTRACT

This paper summarizes the development of an LES based model for reliable description of combustion in a gas turbine combustion chamber. Combustion is described by means of the flamelet generated manifolds (FGM) method. A Smagorinsky-model with dynamic procedure is applied to determine the subgrid scale stresses. A gradient ansatz model is used to represent the sub-grid scale scalar flux in the mixture fraction and in the reaction progress variable equations. Soot formation and radiation are not considered.

In order to evaluate the capability of the model for predicting combustion processes induced by complex real fuels a high pressure single sector combustor (SSC) is investigated. This combustion chamber is fuelled with pre-vaporized kerosene fuel and features very complex unsteady swirling flow and partially premixed combustion properties. The validation of the designed tool along with the prediction analysis is carried out in terms of comparison between experimental data (achieved with a nozzle fired at 0.6 Mpa) and numerical results. This reveals that the proposed LES model is able to capture satisfactorily the flow and combustion properties involving. In particular the flame is predicted to be not always attached to the nozzle. It fluctuates between a lifted and an attached regime. This agrees with experimental findings.

INTRODUCTION

Gas turbine combustion systems are characterized by flows that typically involve various interacting phenomena. These include turbulence, mixing, mass and heat transfer, radiation and multiphase flow. The flows exhibit large scale structures and evolve in a highly unsteady manner, which remains inaccessible to today's RANS (here Reynolds Averaged Navier Stokes based numerical simulations) methods widely used in many 3D CFD industrial simulation tools [1].

Focusing on gas turbine combustion systems, it is worth mentioning, that only a few combustion system designs could be studied and experimentally tested in the past as the cost for combustion testing are expensive. Furthermore, the designs have been optimized for years for steady state [2]. Due to inherent unsteady combustion events, like ignition, relight, quenching, blow out, combustion instabilities that may strongly influence the system operation, the optimization process appears often ineffective.

To take into account inherent unsteady effects, to significantly reduce development costs and to simultaneously meet specific optimization targets (efficiency and emission reduction, safety, fuel consumption reduction, etc.), a reliable design tool is highly demanded [2 - 7]. In this respect, Large Eddy Simulation (LES) that has demonstrated its potential in reasonably simple combustion systems (laboratory flames) is a valuable candidate as a compromise between Direct Numerical Simulation (DNS) and RANS.

Due to rapid development of computer performance and application-oriented numerical methods, computational and programming techniques, the application of LES to technical combustion systems has now been made possible. Recently LES applications have been reported in test cases of high complexity [4, 7 - 11]. Despite these LES successes, its path to become a validated production tool in the industry is still open [12]. Especially the need of accurate combustion models that are able to deal with complex combustion regimes in practical test cases is high.

Physical and chemical features of combustion LES have been discussed by Janicka and Sadiki [1] and Pitsch [13] with emphasis focused on important aspects of an overall model. Thereby an overall LES model formulation may contain physics-preserving turbulence/mixing closures. These include an appropriate combustion sub-model able to capture finite chemistry effects along with a sub-model for turbulence-chemistry interactions, and possible sub-models accounting for additional phenomena, such as multiphase flow phenomena, radiative heat transfer and soot formation, etc. Regarding chemistry, the details of chemistry are unavoidable if one has to address auto-ignition, flame stabilization, recirculation products which may include intermediate species, and the prediction of some pollutants [14 - 16]. The reduction and tabulation of chemical species behavior prior to LES remains one of the available options investigated to downsize combustion chemistry [17]. Recent contributions are reported in this paper.
To account for the stabilization of lifted flames via partial premixing as occurred in the gas turbine combustor, the flamelet generated manifolds (FGM) method is introduced [18,19]. This is achieved by taking into account an additional transport equation for the progress variable in the CFD besides the mixture fraction equation used and the classical governing equations for LES. Soot formation and radiation modeling are not included.

In order to demonstrate the feasibility of such an LES model to complex flows of practical applications, a realistic single sector combustor as experimentally investigated in the frame work of TIMECOP-AE project is used. This combustion chamber is fuelled with pre-vaporized kerosene fuel using a nozzle fired at 0.6 Mpa. It features a strong unsteady swirling flow with recirculation and breakdowns of large scales vertical structures, turbulent mixing, combustion, conjugate heat and mass transfer and pollutant formation. These complex interacting processes make predictions of such a system very complicated and challenging even if only part of the phenomena is considered.

This paper is organized as follows. The governing equations, modeling and computational methods are first reviewed. In particular, the combustion LES model based on the FGM is presented. Then, the details of the test case investigated are briefly described. These are followed by the simulation results obtained in comparison with experimental data. These results are analyzed and discussed. The final section is devoted to the conclusions.

NOMENCLATURE

Latin symbols

Y_α	species concentration of species α
J_i	sub grid scalar flux vector component
t	time
x_i	distance co-ordinate
x,y,z	tangential, radial and axial co-ordinates
u_i	velocity component
M	molecular mass
S_α	source term

Greek Letters

μ	dynamic viscosity
ν	kinematic viscosity
ξ	mixture fraction
ρ	density
σ	Schmidt number
Φ	equivalence ratio
Φ	thermo chemical property
δ	delta-PDF
τ_{ij}	SGS stress (tensor) component
Δ	filter width

Operators

$(\bar{\cdot})$	filtered
$(\tilde{\cdot})$	Favre-filtered

Acronyms:

MOLECULES	MOdeling of Low Emissions Combustors Using Large Eddy Simulation
CFD4C	Computational Fluid Dynamics for Combustion
TIMECOP	Toward Innovative Methods for Combustion Prediction in Aero-Engines

FILTERED GOVERNING EQUATIONS, MODELING AND COMPUTATIONAL METHODS

In this paper, a classical approach for LES is used. To separate the large from small-scale structures in LES, filtering operations are applied to the governing equations, which are the momentum equation (2) along with the continuity equation (1) used to describe the motion of low Mach number Newtonian fluids. In addition, the change of mixture fraction, ξ, caused by the turbulent convection and diffusion of a passive (or conserved) scalar is given by the transport equation (3).

$$\frac{\partial \overline{\rho}}{\partial t} + \frac{\partial \overline{\rho} \tilde{u}_i}{\partial x_i} = 0 \tag{1}$$

$$\frac{\partial}{\partial t}(\overline{\rho}\tilde{u}_i) + \frac{\partial}{\partial x_j}(\overline{\rho}\tilde{u}_i\tilde{u}_j) = \frac{\partial}{\partial x_j}\left[\begin{array}{l} \overline{\rho}\nu\left(\frac{\partial \tilde{u}_i}{\partial x_j} + \frac{\partial \tilde{u}_j}{\partial x_i}\right) - \\ \frac{2}{3}\overline{\rho}\nu\frac{\partial \tilde{u}_k}{\partial x_k}\delta_{ij} - \overline{\rho}\tau_{ij}^{sgs} \end{array}\right] - \frac{\partial \overline{p}}{\partial x_i} + \overline{\rho} g_i \tag{2}$$

$$\frac{\partial}{\partial t}\overline{\rho}\tilde{\xi} + \frac{\partial}{\partial x_i}\left(\overline{\rho}\tilde{u}_i\tilde{\xi}\right) = \frac{\partial}{\partial x_i}\left(\overline{\rho}\tilde{D}_f\frac{\partial \tilde{\xi}}{\partial x_i}\right) - \frac{\partial}{\partial x_i}\left(\overline{\rho}J_i^{sgs}\right) \tag{3}$$

In equations (1)-(3) the quantity u_i (i=1, 2, 3) denotes the velocity components at x_i direction, ρ the density, p the static pressure and δ_{ij} the Kronecker delta. The quantity ν is the molecular viscosity and D_f the molecular diffusivity coefficient.

In order to take into account chemical kinetic effects, the introduction of variables to track the reaction progress is required, especially when the combustion takes place in the partially premixed regime. This is achieved by incorporating an additional transport equation for the reaction progress variable (RPV) into the CFD, besides the mixture fraction equation already available:

$$\frac{\partial}{\partial t}\overline{\rho}\tilde{Y}_\alpha + \frac{\partial}{\partial x_i}\left(\overline{\rho}\tilde{u}_i\tilde{Y}_\alpha\right) = \frac{\partial}{\partial x_i}\left(\overline{\rho}\tilde{D}\frac{\partial \tilde{Y}_\alpha}{\partial x_i}\right) - \frac{\partial}{\partial x_i}\left(\overline{\rho}J_i^{sgs}\right) + \overline{S}_\alpha,\ \alpha = \{1,2,...\} \tag{4}$$

where $\tilde{Y}_\alpha$ is the filtered concentration of the reaction progress variable α. The quantity D denotes the molecular diffusivity coefficient. For the combustion process under investigation the Y_α has been defined as a (linear) combination of reaction product species:

$$Y_\alpha \equiv Y_{RPV} = \frac{Y_{CO_2}}{M_{CO_2}} + \frac{Y_{H_2O}}{M_{H_2O}} + \frac{Y_{H_2}}{M_{H_2}} \tag{4b}$$

where Y_i and M_i denote the mass fraction and the molar mass of the species i, respectively. Equations (1)-(4) govern the evolution of the large, energy-carrying scales of flow and mixing field denoted by an over-bar. In the flow and scalar field, the effect of the small scales appears through the SGS stress tensor and the SGS scalar flux vector,

$$\tau_{ij}^{SGS} = \widetilde{u_i u_j} - \tilde{u}_i\tilde{u}_j \tag{5}$$

$$J_i^{sgs} = \widetilde{u_i z_\alpha} - \tilde{u}_i\tilde{z}_\alpha, \quad z \equiv (\xi, Y_\alpha) \tag{6}$$

respectively. The last term, $\overline{S}_\alpha$ in equation (4) is the filtered chemical reaction rate. This together with the SGS stress tensor and scalar flux vector (5,6) must be modeled in order to obtain a closed system of equations (1) - (4).

A Smagorinsky-model with dynamic procedure according to Germano et al. [20] is applied to determine the subgrid scale stresses. In order to stabilize the model, the modification proposed by Sagaut [21] is applied. In addition a clipping approach will reset the negative Germano coefficient C_s to zero to avoid destabilizing values of the model coefficient. No special wall-treatment is included in the sub grid scale model. The dynamic procedure applied here allows to capture the correct asymptotic behavior of the turbulent flow when approaching the wall (see e.g. Wegner et al., [22]). A detailed discussion of this issue was reported by Wegner [23]. To represent the sub-grid scale scalar flux in the mixture fraction and in the RPV equations a gradient ansatz (6b) is applied with a constant turbulent Schmidt number of 0.7.

$$J_i^{sgs} = -\frac{\upsilon_t}{\sigma_t}\frac{\partial \tilde{z}}{\partial x_i} \quad \upsilon_t = C_s\Delta^2\left|\tilde{S}\right| \tag{6b}$$

υ_t is the turbulent viscosity, Δ is the filter width, σ_t the turbulent Schmidt number and $\left|\tilde{S}\right|$ the absolute value of the strain rate. Although advanced sub grid scale scalar flux models exist and are known to behave superior in specific flow test cases (Huai et al. [24]), the model combination described above and applied here was chosen due to its simplicity.

The remaining term to be closed, i.e. the chemical reaction term, is modeled following the FGM method [18]. As any flamelet based model, flamelet generated manifolds are based on the idea that a multi-dimensional flame can be represented by a set of one-dimensional flamelets. The method is therefore based on the laminar flamelet equation and includes Intrinsic Low-Dimensional Manifold (ILDM) [25] reduction methodo-

logy by solving transport equations for a given number of progress variables. Note that premixed and non-premixed generated manifolds can be constructed, even they can be combined. A comparative study has been reported in [26] for an LES of Sandia flame D and F. Visual observation from experiments show that the flame featuring both lifted and attached behavior exhibiting partially premixed combustion properties. Instead of considering diffusion flamelets, the FGMs used in this work are based on steady 1-D premixed flames to capture the lifted flame behavior. One reaction progress variable as defined in equation (4b) is used. In the following it is labeled $Y_1 \equiv y$. Because of the swirled air a strong variable local equivalence ratio occurs within the test cases. This is taken into account by introducing a mixture fraction variable as described by equation (3).

According to this approach a Favre-filtered thermo-chemical quantity, ϕ, is calculated by integrating over the joint PDFs of the mixture fraction and the RPV while accounting for the turbulence-chemistry interaction

$$\tilde{\phi} = \int_0^1 \int_0^1 \phi(\xi, y^*) P(\xi, y^*) dy^* d\xi \tag{7}$$

In equation (7), a quantity labeled as (*) expresses a normalized quantity by its value at chemical equilibrium, and the instantaneous thermo-chemical quantities are provided in a detailed chemistry table as described by Wegner [23] and Vreman et al. [26].

Since the normalized reaction progress variable is assumed to be statistically independent from the mixture composition, the unknown PDF can be split up as a product of two single-variable PDFs, for the mixture fraction and the progress variable, respectively. Each one-variable PDF is then assumed to have a presumed form. For the mixture fraction, we employ the Beta-form determined by the filtered mean value and the variance. For the PDF of progress variable in premixed and partially premixed flame, it is expected that two strong peaks can occur at y*=0 and y*=1. Although a better approximation would be a three delta peak PDF, a delta-function only determined by the filtered mean of the RPV is chosen for the RPV as a crude first-order approximation in the context of the present work. A first evaluation of this approximation can be gained from the prediction of possible lift-off distances. This consideration leads to:

$$P(\xi, y^*) = P(\xi) \bullet P(y^*) \tag{8}$$

$$P(\xi, y^*) = \beta(\xi; \tilde{\xi}, \widetilde{\xi''^2}) \bullet \delta(\widetilde{y^*}) = P(\xi; \tilde{\xi}, \widetilde{\xi''^2}, \widetilde{y^*}) \tag{9}$$

A discussion of the issue of statistical independence has been carried out in the literature and can be found in [16]. According to equation (9) the thermo-chemical quantities can then be parameterized and tabulated in the so-called pre-integrated tables (tabulated SGS chemical parameters) as function of the filtered mixture fraction, its variance and the normalized filtered RPV:

$$\tilde{\phi} = f(\tilde{\xi}, \widetilde{\xi''^2}, \widetilde{y^*}) \tag{10}$$

Instead of solving a transport equation for the mixture fraction variance, mixture fraction variance is obtained according to a simple gradient formulation as a first approximation. The work by Kempf [27] has shown that good predictions of a wide variety of different flames can be achieved using the presumed PDF approach with algebraic modeling of the variance. Thereby the mixture fraction variance is calculated by

$$\widetilde{\xi''^2} \approx C_{eq} \Delta^2 \frac{\partial^2 \tilde{\xi}}{\partial x_i^2} \tag{11}$$

In the present work the coefficient C_{eq} is set to 0.15

Since kerosene is used as fuel, its chemical composition in the FGM context is represented by a model fuel consisting of 80% n-decane and 20% n-propylbenzene (by volume), which should represent two different chemical groups: long chained alkanes as the major component and cyclic hydrocarbons as the second large group. This model fuel was developed within the EU project CFD4C [28]. It has been validated against measurements of ignition delay times and burning velocity. The mechanism consists of 180 species and 992 reversible reactions.

To note that, the FGM approach is the same for both kerosene and methane fuels. First validation case was performed for methane fuel in complex geometries [32] in the frame work of MOLECULES project [29] (see also [23, 26]). In that sense, it is a general approach that can be applied to any fuel. There are no different strategies or specific issues for kerosene. This is a strong advantage of the method.

All the governing equations have been implemented in the three dimensional CFD code, FASTEST-3D. The code uses geometry-flexible, block-structured, boundary fitted grids. This enables to represent complex geometries. A collocated grid with a cell-centered variable arrangement is used. The flow solver offers fully second order accuracy. Discretization is based on finite volume method. For spatial discretization specialized central-differencing schemes are used. To assure boundedness of the mixture fraction, the convective term in the scalar transport equations has been discretized using non-oscillatory bounded TVD (Total Variation Diminishing) schemes [30]. For the time stepping multiple stage Runge-Kutta schemes with second order accuracy are used. Following a fractional step formulation, in each stage a momentum correction is carried out in order to satisfy the continuity. FASTEST is parallelized by domain decomposition using the MPI message passing library. This code has been already used to study numerically a series of laboratory classical flames [22, 23, 31] and a generic combustor fueled by methane using FGM method for combustion [22, 23,

31]. Computations are carried out for three flow throughs prior to collecting statistics and four flow throughs for obtained time averaged values.

TEST CASES AND BOUNDARY CONDITIONS

The aim of the experiments conducted in the frame of TIMECOP-AE was to replace natural gas used in previous test cases [32] by pre-vaporized liquid kerosene. A set-up designed by DLR (Deutsches Zentrum für Luft- und Raumfahrt) was used for the fuel supply, where liquid kerosene was vaporized at a minimum temperature of 673 K in a flowing system. To achieve comparable conditions for mixing and combustion with previous methane based studies [23, 32] a primary combustion chamber pressure of at least 0.4 Mpa was necessary to supply sufficient momentum for the fuel-jet in the actual test cases. It consists of a squared cross section single sector combustor (SSC) as depicted in Fig. 1, where combustion air was supplied through a swirl nozzle. It is optically accessible from three sides in order to allow various modern optical laser diagnostics. The test rig can withstand an operating pressure of up to 2 Mpa and can be operated with a combustion air flow up to 1.3 kg/s and cooling air flow rates of up to 3.0 kg/s. The maximum heating temperature of the combustion air is 850 K. Similar to the previous combustion chamber, the fused silica windows of the combustion chamber are cooled by guided cooling air, which is let into the hot exhaust before leaving the combustor through a throttling nozzle. In order to keep further disturbances of the chemical and physical reactions inside the combustion chamber small, no secondary air was used (Fig. 1) in the experiments. Note that the "combustion air" inlet supplies the swirler/injector part, while a "window air" inlet provides fresh gas through films on the front combustion chamber wall. This air entering the main combustion chamber is needed during the experiment to avoid any soot deposition on the windows impacting the optical quality. In computations the window air was not included. The SSC test rig pressure is controlled by the amount of cooling air let into the system. In the present test case, dilution of hot gases by cold air is not considered for both experimental and numerical studies.

Flow fields and flame stabilization were investigated using state-of-the-art Laser Doppler velocimetry (LDV) and planar laser-induced fluorescence (PLIF) methods. This paper focuses on validation of the model implemented in the in-house CFD code FASTEST-3D and does not give details of the spectroscopic part of the measurements, consisting of kerosene LIF, OH-LIF and chemiluminescence measurements at three different operating points. In fact, the fired nozzle was operated at 0.4, 0.6 and 0.9 Mpa, with an air mass flow of 77, 114 and 170 g/s heated up to 623K, corresponding to a pressure drop across the nozzle of 3.4% for all three investigated test cases.

Nozzle swirl number (geometrical)	1.2
Combustor pressure [Mpa]	0.6
Fuel	Pre-vaporized kerosene Jet -A1(Experiments)
	80% n-decane and 20% n-propylbenzene (FGM)
Kerosene mass flow rate(g/s)	6.12
Fuel temperature [K]	673
Oxidant	Air
Mass flow of Oxidant [g/s]	114
Oxidant Temperature [K]	623
Equivalent ratio	0.9
Thermal Power (kW)	250
AFR(Air Fuel Ratio)	18.6

Table 1: Operating conditions

The global equivalence ratio was set to ϕ= 0.9 which is equal to an Air Fuel Ratio (AFR) of 18.6. As a result, a comprehensive database including, the velocity flow fields and the characteristic parameters of the flame derived from the spectroscopic measurements has been provided. This database is suitable for model validation and numerical simulation. For the present investigations, the test case corresponding to a combustion chamber pressure of 0.6 Mpa is considered. Table 1 summarizes the corresponding operating conditions.

To simulate the configuration as shown in Fig. 1 the computational domain in Fig. 2 is considered. It includes the combustion chamber and the swirl nozzle represented by a mesh consisting of 137 grid blocks featuring an O-type structure. The total number of grid points is 2.0 millions. The resulting mesh is able to resolve more than 85% of total kinetic energy of the flow field in accordance to the so-called Pope-criteria (see in [1]). All simulations were run on sixteen processors.

As inlet boundary conditions, the mass flows from the experiment were prescribed using laminar unperturbed profiles. A laminar inlet profile used was sufficient for such a simulation as measurements from experiments show that flow field is dominated by the intense recirculation of the swirl flow and not by the inlet turbulence [23].

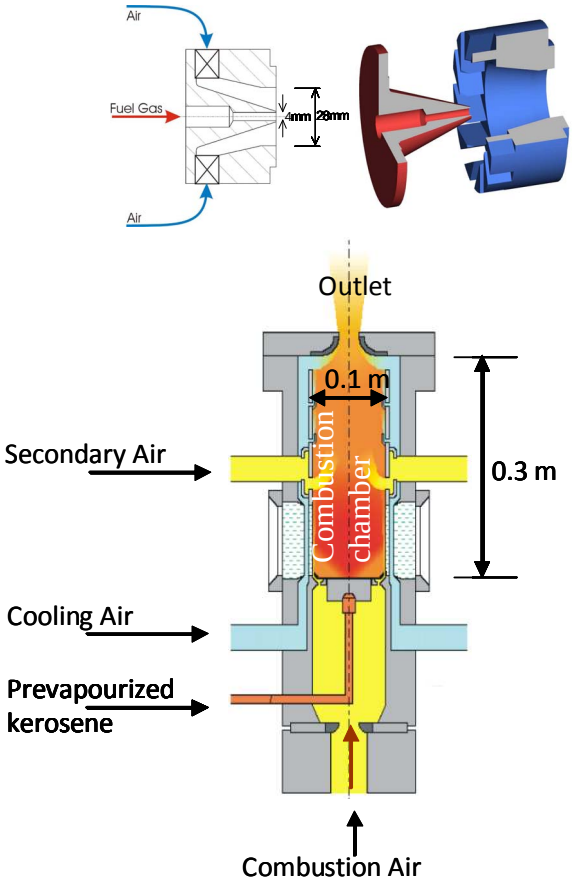

Figure 1: Experimental setup (bottom) and swirled nozzle (top)

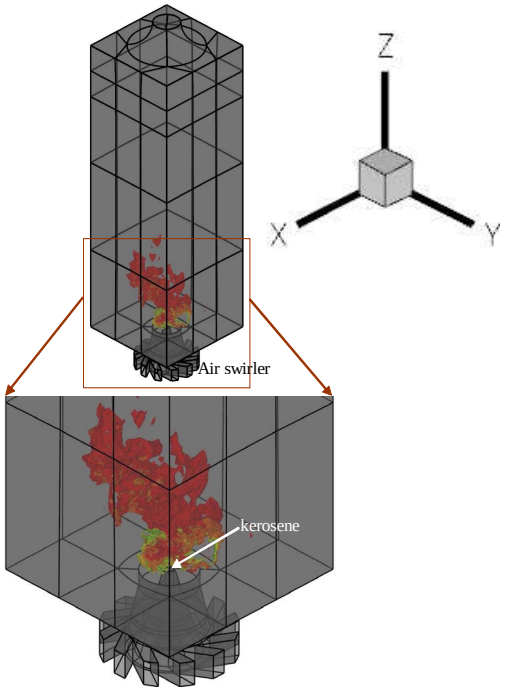

Figure 2: Computational domain with instantaneous isosurfaces of the reaction source term

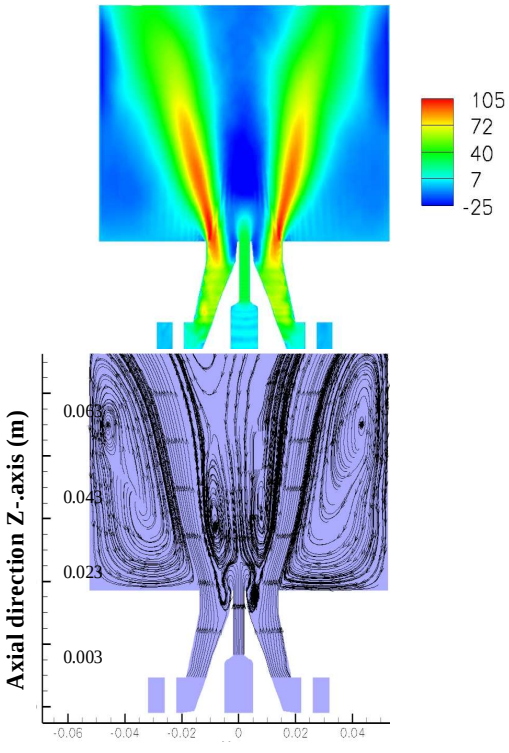

Figure 3: Time averaged axial velocity magnitude (m/s) (top) and time averaged velocity streamlines computed from LES (bottom).

RESULTS AND DISCUSSIONS

In this section we present some numerical results obtained for the kerosene pre-vaporized combustion for the 0.6 Mpa case. Flow field results will be discussed first, followed by an analysis of some flame characteristics.

The time averaged velocity magnitude and streamlines resulting from the simulation are shown in Fig. 3. Negative velocities are seen on top of kerosene jet and also surrounding it, leading to limit the kerosene fuel jet penetration depth within few millimeters from the exit of the nozzle. Negative velocities are also observed in the air swirler side near exit of the nozzle. This is leading to a partial infiltration of kerosene into the nozzle. The main feature of the flow is the spreading of the flow, surrounding a reverse flow area reaching back to the stagnation point. The recirculation zone along the centerline reaches down to a stagnation point at x, y, z = 0, 0, 6 mm and grows from a diameter of 8 mm at x= 10 mm to a diameter of 16mm at x = 20mm away from the nozzle. This can also be seen in Figs. 4 and 5. The recirculation zone is typical for highly swirling flows and results from a positive axial pressure gradient that is associated with the vortex breakdown phenomenon. The highest positive (negative) axial velocity occurred at x, y, z = 0, 12, 5 mm, (0, 0, 20) mm, where a velocity of 76 m/s (-18 m/s) was

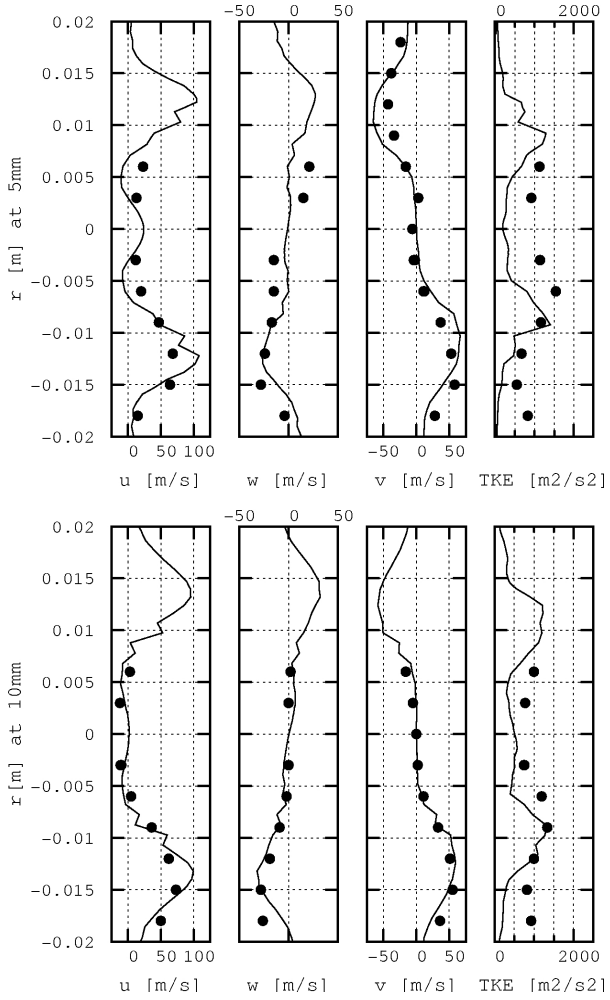

Figure 4: Radial profiles of time averaged axial (u), radial (w) and tangential (v) velocity components and turbulent kinetic energy (TKE) at 5 mm (top) and 10 mm from the exit of the nozzle (__simulated , •Exp)

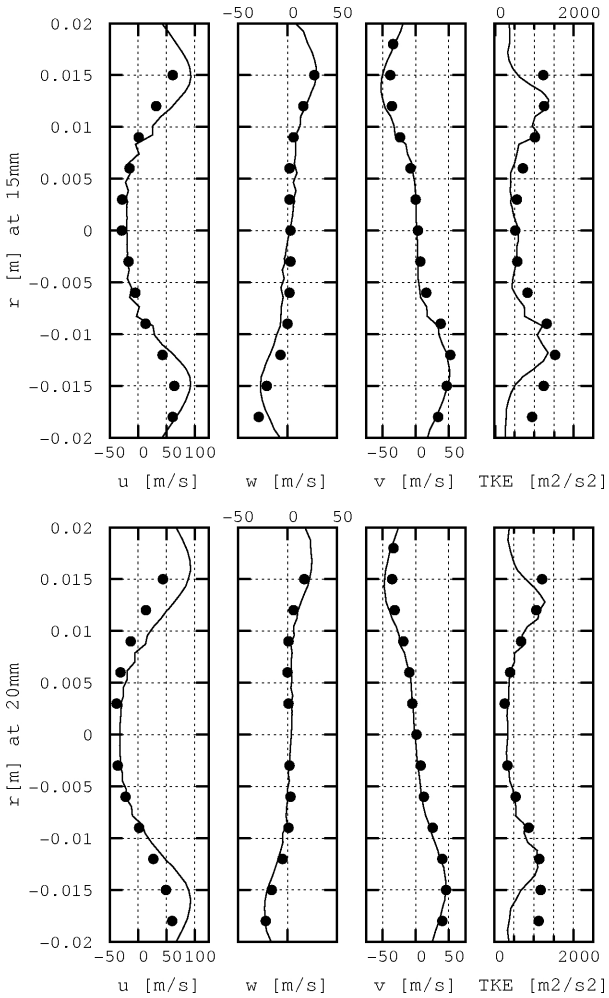

Figure 5: Radial profiles of time averaged axial (u), radial (w) and tangential (v) velocity components and turbulent kinetic energy (TKE) at 15 mm (top) and 20 mm from the exit of the nozzle (__simulated , •Exp)

measured. The highest radial velocity was 31 m/s at x, y, z = 0, -18, 15 mm, whereas the highest tangential velocity reached up to 59 m/s at x, y, z = 0, -12, 5 mm. As pointed out above this observation can also be made from Fig. 4 and 5 in which velocity profiles and turbulent kinetic energies are plotted at different axial positions from the nozzle exit (x = 5 and x = 10 mm in Fig. 4 and; x = 15 and x = 20 mm in Fig. 5). All three components of the velocities and the turbulent kinetic energy predicted by the LES are in good agreement with the experimental data. The axial velocity component is becoming strongly negative from x = 5 mm to x = 20 mm away from nozzle exit. This indicates the presence of a recirculation zone, which is necessary for flame stabilization.

In this respect, the instantaneous RPV source term, the CO mass fraction and the temperature plotted in Fig. 6 (top) and time averaged values of the RPV source term, the RPV source variance and the temperature in Fig 6 (bottom) allow to give a first impression of the flame characteristics.

The instantaneous RPV source term in Fig. 6a is located in the main reaction zone. The flame seems to stand above the nozzle featuring a lifted flame in agreement with experiments. However it can be observed from the averaged reaction progress variable source term plotted (Fig. 6.e) that the flame is attached to the nozzle, though the value of the RPV source term remains very low. This suggests that the flame may be fluctuating between an attached and a lifted regime. In non-premixed swirled combustion as investigated in [23] the flame was found to be lifted while exhibiting a partially premixed nature. The RPV source term variance plotted in Fig 6.f looks like two thin leafs starting from the swirled nozzle tip. It is

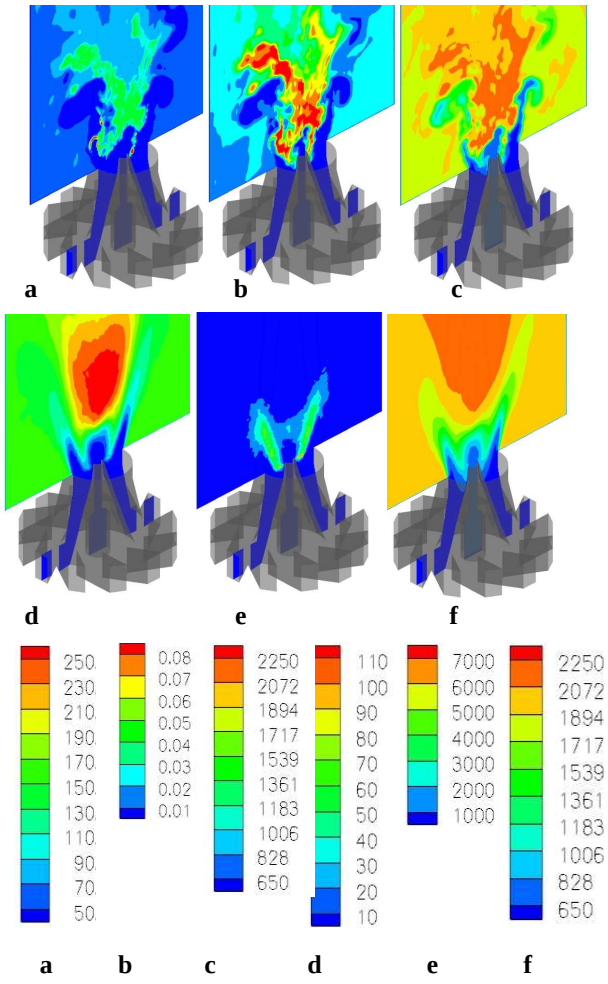

Figure 6: Contour plots of instantaneous (top) and time averaged (bottom) a) RPV source (kg/m^3-s) b) CO mass fraction c) temperature (K) d) source term (kg/m^3-s) e) RPV resolved source variance f) temperature (K) on a plane passing through the centre of nozzle

worth noting that the reaction progress variable is strongly influenced by the swirl flow. This causes the strong change of the RPV in the mixing layer of the swirled air flow and the fuel. Especially it is observed that higher values of the RPV variances are disappearing above distances x = 10 mm away from the nozzle exit.

A high concentration of CO in the reaction zone is observed in Fig 6.b. Most of the CO is combusting further downstream to limit the reaction zone within the vicinity of the nozzle. This is strongly influenced by the swirled air. The maximum instantaneous temperature in the reaction zone is found to be 2250 K (Fig 6.c). This maximum temperature is found at stoichiometric mixture fraction region. Averaged and instantaneous temperature contours in Fig 6.c and f,

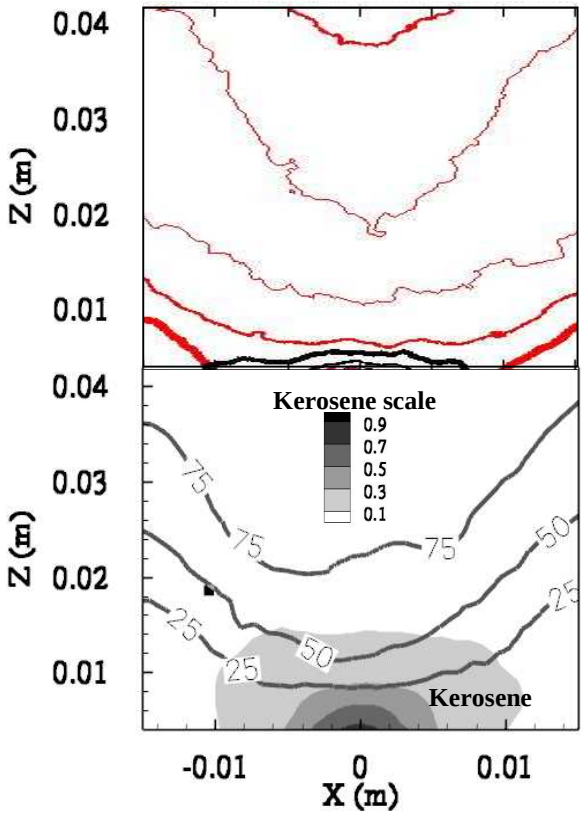

Figure 7: Qualitative representaion of OH concentration and kerosene. Top: Experiment (bold contour: 25% of maximum; middle contour: 50% of maximum; light contour: 75% of maximum). Bottom: simulation

respectively, confirm that the main reaction zone of the flame is lifted. Streamline plots derived from experimental LDV data as well as from numerical simulation show the existence of a recirculation zone responsible for stabilization of the flame and a fluctuating stagnation point near the nozzle, causing the flame position to also fluctuate between a lifted to an attached behavior.

A comparison of predicted mass fraction of OH species and kerosene by LES against pixel intensity from experiments is shown in Fig. 7 for the main reaction zone region. The different red line contours of Fig. 7 (top) show the distributions of averaged OH measured in experiments. Gray line contours of Fig. 7 (bottom), with corresponding percentage of time averaged maximum OH mass fraction are estimated by LES. Experiments show the maximum OH concentration on top the fuel jet. This is also confirmed by LES. In general, though OH mass fractions from the LES calculations are qualitatively comparable with those from experiments, they differ from each other by a few millimeters in physical space. One of the reasons may be the window air effect that was not included in computations. In particular the greater part of the vaporized

kerosene (dark lines in Fig 7 (top)) that is located in the vicinity of the nozzle is captured by the LES (gray scale contours of Fig 7 (bottom)) with a slight deviation.

Due to the lack of detailed experimental data regarding the other species concentration and a temperature distribution an appropriate assessment of the model with respect to this prediction could not be provided.

CONCLUSIONS

An LES based advanced combustion model for a reliable description of combustion processes in a gas turbine combustion chamber has been developed and implemented in the FASTEST-3D code. The numerical approach including a FGM method based combustion model was successfully assessed with respect to its prediction capability of the flow and combustion characteristics. In particular the complex flow field properties in the SSC are captured well. However, it could be pointed out that turbulent kinetic energy at 5 mm from exit of the nozzle is not in agreement with the experimental data. The results further show that the flame is not always attached to nozzle and appears to fluctuate in time. The remaining test cases (0.4 and 0.9 Mpa cases) and further investigations in terms of sensitivity studies with respect to inflow conditions and grid are to be analyzed in future work.

ACKNOWLEDGMENTS

"This work received funding from the European Community through the project TIMECOP-AE (Project # AST5-CT-2006-030828). It reflects only the author's views and the Community is not liable for any use that may be made of the information contained therein."

REFERENCES

[1] Janicka, J., and A. Sadiki. A. (2005), “Large eddy simulation of turbulent combustion systems”. Proc. Comb. Inst., 30:537-547.

[2] Patel, N., Kirtas, M., Sankaran, V. and Menon, S. (2007), “Simulation of spray combustion in a lean-direct injection combustor”, Proc. Combust. Inst., 31 (2) , pp.2327–2334.

[3] Boudier, G., Gicquel, L., Poinsot, T., Bissieres, D. and Berat, C. (2007), “Comparison of LES, RANS and Experiments in an aeronautical gas turbine combustion chamber”, Proc. of Comb. Inst., 31 (2), pp. 3075-3982.

[4] Boudier, G., Staffelbach, G.., Gicquel, L., and Poinsot, T. (2007b), “Reliability of large eddy simulateion of combustion in complex test cases”, Proc. of Workshop “Quality and Reliability of LES”, 24-26 October 2007, Leuven, Belgium.

[5] Vervisch, L., Domingo, P., Lodato, G., Veynante, D., (2010), “Scalar energy fluctuations in Large-Eddy Simulation of turbulent flames: Statistical budgets and mesh quality criterion”, Combustion and Flame, 157(4).

[6] Wang, H., Stephen B.P. (2011), “Large eddy simulation/probability density function modeling of a turbulent CH4/H2/N2 jet flame”, Proceedings of the Combustion Institute, Volume 33, Issue 1, 2011, Pages 1319-1330.

[7] Moin, P., Apte, S.V., (2006), “Large Eddy Simulation of Realistic Gas Turbine Combustors”, AIAA Journal, 44 (4), pp. 698-708.

[8] Fureby C., Grinstein, FF., Li, G., and Gutmark, E.J. (2007), “An experimental and Computational study of a multi-swirl gas turbine combustor”, Proc. Of the Combustion Institute, 31, pp. 3107-3114.

[9] Staffelbach G., Gicquel L., and Poinsot T. (2005), “Highly parallel large eddy simulations of multiburner test cases in industrial gas turbines”, The Cyprus international Symposium on complex effects in LES.

[10] Vermorel, O., Richard, S., Colin, O., Benkenida, A., Angelberger, C., and Veynante, D. (2007), “Multi-Cycle LES Simulations of Flow and Combustion in a PFI SI 4-Valve Production Engine”, SAE Technical paper series, 2007-01-0151.

[11] Jones, W.P., Lyra, S., Navarro-Martinez S., (2011), “Large Eddy Simulation of a swirl stabilized spray flame”, Proceedings of the Combustion Institute, Volume 33, Issue 2, 2153-2160.

[12] James, S., Zhu, J. and Anand, M.S. (2006), “Large Eddy Simulations as a Design Tool for Gas Turbine Combustion Systems”, AIAA Journal, 44 (4), pp. 674-686.

[13] Pitsch, H. (2006), “Large Eddy Simulation of Turbulent Combustion”, Ann. Rev. Fluid Mech., (38) (2006), pp. 453–482.

[14] Warnatz, J., Maas U., and Dibble RW. (1996) “Combustion”, Springer Verlag.

[15] Pope. S.B. (2000), “Turbulent Flows”, Cambridge Universtiy Press, Cambridge.

[16] van Oijen, J.A., Bastiaans, R.J.M., and de Goey, L.P.H. L.P.H. (2007), “Low-dimensional manifolds in direct numerical simulations of premixed flames”, Proc. Combust Inst., 31 (2), pp. 1377–1384.

[17] Vervisch, L., Lodato, D. and Domingo, P., (2007) Proc. of Workshop „Quality and Reliability of LES“, 24-26, October 2007, Leuven, Belgium.

[18] Van Oijen, J.A., De Goey, L.P.H. (2000) , "Modelling of Premixed Laminar Flames using Flamelet-Generated Manifolds",Combustion Science and Technology. 161,113-137.

[19] van Oijen, J.A., de Goey, L.P.H. (2004) , “A numerical study of confined triple flames using a flamelet-generated manifold”, Combust. Theory Modeling, 8(1), 141-163, (2004).

[20] Germano M., Piomelli U., Moin P., and Cabot W. H., 1991, “A dynamic sub-grid scale eddy viscosity model”, Physics of Fluids, A(3): pp 1760-1765.

[21] Sagaut, P., (2001), “Large Eddy Simulation for incompressible Flows”, Springer, Berlin.

[22] Wegner, B. Maltsev, A., Schneider, C., Sadiki, A., Dreizler, A., Janicka, J. (2004), “Assessment of unsteady RANS in predicting swirl flow instability based on LES and Experiments. International Journal of Heat and Fluid Flow”, 25:528-536, 2004.

[23] Wegner, B. (2007), “A Large-Eddy Simulation Technique for the Prediction of Flow, Mixing and Combustion in Gas Turbine Combustors”. PhD thesis, Technische Universitaet Darmstadt, VDI Verlag GmbH, ISBN 978-3-18-354906-1.

[24] Huai, Y., Sadiki, A. (2006), “Analysis and optimization of turbulent mixing with large eddy simulation”, In: ASME 2nd Joint U.S.-European Fluids Engineering Summer Meeting, FEDSM 2006-98416, Miami.

[25] Maas U. and Pope S. B.(1992), “Simplifying Chemical Kinetics: Intrinsic Low-Dimensional Manifolds in Composition Space”, Combust. and Flame, 88, 239-264.

[26] Vreman, A.W., Albrecht, B.A., van Oijen, J.A., de Goey, L.P.H. and Bastiaans, R.J.M. (2008) “Premixed and non-premixed generated manifolds in Large-eddy simulation of Sandia flame D and F”, Combustion and Flame, 253, pp. 394-416.

[27] Kempf, A. (2003), Large-Eddy Simulation of Non-Premixed Turbulent Flames, Ph.D. thesis, Darmstadt University of Technology.

[28] Final Report (2003), Computational Fluid Dynamics for Combustion (CFD4C), CEC Project No: GRD1-1999-10325.

[29] Final Report (2004), “Modeling of Low Emissions Combustors using Large Eddy Simulations, (MOLECULES)”, EC Project GRD1-2000-25221.

[30] Waterson.N. P and Deconinck. H(1994), "Development of bounded higher-order convection scheme for general industrial applications", Project Report 1994-33, Von Karman Institute.

[31] Ketelheun.A, Olbricht. C, Hahn.F, Janicka. F(2010), "NO prediction in turbulent flames using LES/FGM with additional transport equations", Proceedings of the Combustion Institute, Volume 33, Issue 2, 2011, Pages 2975-2982.

[32] Janus, B., Dreizler, A., Janicka, J. (2006), “Experiments on swirl stabilized non-premixed natural gas flames in a model gas turbine combustor”, Proc. Comb. Inst., 31.